Inverse Determination of Eroded Smelter Wall Thickness Variation Using an Elastic Membrane Concept

Daniel Baker
P. O. Box 124,
Lemont, PA 16851

George S. Dulikravich[1]
Professor
Department of Mechanical and Materials Engineering,
Multidisciplinary Analysis, Inverse Design, Robust Optimization and Control (MAIDROC),
Florida International University,
10555 West Flagler Street,
EC 3474, Miami, FL 33174
e-mail: dulikrav@fiu.edu

Brian H. Dennis
Department of Mechanical and Aerospace Engineering,
University of Texas at Arlington,
UTA Box 19018,
Arlington, TX 76019

Thomas J. Martin
Pratt & Whitney Engine Company,
Turbine Discipline Engineering and Optimization Group,
M/S 169-20,
400 Main Street,
East Hartford, CT 06108

A novel algorithm has been developed for the nondestructive determination of the shape of the interface between a melt and a refractory material wall in smelter furnaces. This method uses measurements of temperature and heat flux at a number of points on the outer surface of the furnace, and assumes that the inner (guessed) surface of the furnace wall is isothermal. The temperature field is then predicted in the entire furnace wall material by numerically solving a steady state heat conduction equation subject to the measured temperature values on the external surface and the isothermal melt material solidus temperature on the inner surface of the wall. The byproduct of this analysis is the computed heat flux on the external surface. The difference between the measured and the computed heat fluxes on the outer surface of the furnace is then used as a forcing function in an elastic membrane motion concept to determine perturbations to the inner (melt-refractory) surface motion. The inverse determination of the melt-refractory interface shape can be achieved by utilizing this algorithm and any available analysis software for the temperature field in the refractory wall. The initial guess of the inner shape of the wall can be significantly different from the final (unknown) wall shape. The entire wall shape determination procedure requires typically 5–15 temperature field analyses in the furnace wall material. [DOI: 10.1115/1.4000436]

Keywords: inverse problems, shape determination, refractory wall, wall erosion, shape design, hearth wear

1 Introduction

AQ: #1

Walls of furnaces that contain molten materials (metal, glass, etc.) are made of layers of bricks of high-temperature resistive refractory material. High thermal gradients inside the melt create very strong circulations of the melt that causes erosion of the inner wall surface of the furnace. This erosion can lead to the complete depletion of the protective refractory material at certain locations of the furnace wall. At such points, the molten material can easily soften the outer steel casing of the furnace and break it, causing a major industrial disaster. It is therefore highly desirable to continuously monitor the actual thickness of the entire furnace wall so that the furnace can be shut down and the wall material repaired before the breakout happens. The use of any sensors imbedded in the inner surface of the wall (the melt-wall interface surface) is unacceptable because the strong melt velocity field would wash such sensors away very quickly. One method for the determination of the refractory wall thickness utilizes nondestructive measurement techniques and inverse shape determination concepts. Notice that this class of inverse problems is fundamentally different from inverse problems dealing with the determination of unknown boundary conditions on a known geometry [1,2].

Shape inverse determination involves the ability to determine the shape of a configuration satisfying the governing field equation(s) subject to specified surface boundary conditions and certain geometric constraints. A multitude of shape inverse determination techniques have been developed in various fields of science and engineering. Several research teams in countries with strong steel industries have been working on developing and applying such nondestructive monitoring technologies.

Some of the pioneering work was performed in Japan. Yoshikawa and co-workers [3–5] considered axisymmetric configurations of blast furnaces. They attempted to incorporate the effects of the solidified melt layer in their inverse formulation, based on the use of boundary element methods for heat conduction analysis, and a shape optimization algorithm that could handle only a relatively small number of design variables. Shin and Lee [6] used an inverse formulation of a nonlinear heat conduction equation, while Takatani et al. [7] used three-dimensional computational fluid dynamics to predict the temperature field in the wall and consequently the wall erosion topology.

Another significant effort in the development of inverse methods for the determination of the inner wall surface shape was performed in the ex-USSR (Ukraine) by a research team of Matsevity [8–11]. It is concerned with the bottom of the flash smelting furnace, which is the multilayer structure consisting of refractory and heat-insulating materials. Two upper layers are built from chromomagnesite bricks and act as working and insulating lining. Underneath are the layers of refractory bricks and light refractory bricks, which are the heat insulators. The lower refractory brick layer lies on the concrete raft, which is cast on the horizontal steel plate that leans against the columnar concrete supports of the furnace foundation. The width of the wall domain in this problem is much larger than the wall thickness, practically symmetric, relative to the transverse axis, and has a low heat conductivity of the component materials. These facts were used to justify the assumption of the two-dimensionality of the temperature field in the furnace bottom wall. Apparently, this team has not considered a simultaneous prediction of the inner surface of the furnace bottom and sidewalls.

[1]Corresponding author.

Contributed by the Heat Transfer Division of ASME for publication in the JOURNAL OF HEAT TRANSFER. Manuscript received September 21, 2008; final manuscript revised September 17, 2009; published online xxxxx-xxxxx-xxxxx. Assoc. Editor: Yogesh Jaluria.

Preuer et al. [12], Druckenthaner et al. [13], and Radmoser [14], in the Austria/Germany region of central Europe, reported on a more mathematically involved method of simultaneously determining the thickness of the bottom and the sidewall of the blast furnaces that involved the use of a regularization technique, in order to prevent the ill-posed inverse problem from developing exponentially large errors. However, their approach did not appear to be flexible enough to treat realistic irregular inner wall surface configurations.

Sorli and Skaar [15] from Norway reported on a very exact and mathematically sound inverse methodology that converges quite rapidly because it utilizes an adjoint operator formulation. However, the method was demonstrated only for very simple smooth shapes of the inner surface of the wall that were not significantly different from the initially guessed wall surface configurations.

The team of Tanaka [16,17] utilized a sophisticated Kalman filtering technique and boundary element method to deal with axisymmetric configurations of the blast furnaces. Katamine et al. [18], also from Japan, developed a method based on the distributed sensitivity function that uses adjoint variables. Their approach is able to predict quite realistic shapes of the inner surface of the furnace walls, but does not seem to offer a consistently high accuracy in the prediction of the wall wear configuration.

Huang et al. [19] and Roldan [20] in the United States recently reported efforts to predict the configuration of an eroded smelter hearth wall using computational fluid mechanics and an inverse heat conduction approach.

It should be pointed out that despite the separate efforts of several independent research teams, none of the published work utilizing different inverse shape determination approaches has been demonstrated to work reliably when realistic values of temperature and heat flux measurement errors are included. In conclusion, reliable and affordable methodology for continuous sensing and monitoring of realistic three-dimensional variation in refractory wall thickness in smelters is still unavailable. Those available are the several methods for the prediction of the furnace wall thickness variation in a two-dimensional horizontal or vertical plane, assuming a perfect symmetry of the furnace inner and outer walls with respect to the vertical axis.

Furthermore, the existing methods do not offer simultaneously high accuracy, reliability, and speed of the prediction of the wall thickness distribution. The objective of this paper is to elaborate on an alternative method for predicting realistic two-dimensional furnace wall wear configurations reliably and accurately. The new method [21] is based on the authors' concept for inverse design of aerodynamic shapes [22–24] and could be conceptually extended to three dimensions [22].

2 General Approaches to Inverse Determination of Shapes

There exists a multitude of inverse techniques that are useful in solving different types of engineering problems. Two major classes of inverse tools for shape determination can be defined as methods with coupled field analysis and shape modification, and methods with uncoupled field analysis and shape modification. The coupled methods require an intimate understanding of the original field analysis code in order to make specific changes in the boundary condition enforcement subroutines. This is time consuming and hard to accomplish if the original analysis code is not well documented and if the original developers are not available. When a designer uses a commercially available analysis code, he/she cannot perform its conversion to an inverse shape determination code since only a compiled version of the code is available.

The uncoupled inverse methods require no modification to a field analysis code. Thus, any reliable field analysis code or even experimental field measurements data can be used in the shape determination process, without a need for alterations of such a field analysis tool. The field analysis code will be called during the inverse shape determination process as a large subroutine to compute boundary values of certain field variables. These boundary values will then be fed into the master inverse shape determination code that will compute new geometry updates. This means that even a compiled version of a commercially available field analysis code is perfectly acceptable, since it requires only the updated geometry computed by the inverse shape determination master code. This entire procedure constitutes one iteration in the global inverse shape determination process. The uncoupled shape determination techniques have the added benefits of simplicity, relative ease of programming, and versatility.

3 Thermal Boundary Conditions

The essence of all inverse shape determination algorithms is that they require the boundary conditions for field problems to be overspecified on at least some portions of the known part of the boundary. In the problem of inverse determination of the inner surface of the refractory wall in smelters, this means that both temperature T_o and normal temperature derivatives $(dT/dn)_o$ should be provided on the external surface of the refractory wall. A continuous reading of temperature T_o on this surface can be accomplished by placing inexpensive and reliable temperature measuring probes on the outer surface of the furnace refractory wall. The normal derivatives of temperature on the outer surface of the refractory wall of a blast furnace could be measured inexpensively by placing another temperature probe, a few centimeters radially inward from each of the outer surface temperature probes. The difference between the temperatures read by each probe in such a pair of temperature probes can be divided by the known distance between the two probes in a pair to provide the needed outer surface local normal temperature gradient. Values of T_o and $(dT/dn)_o$ can then be interpolated at other surface points by using, for example, B-splines.

The inner surface of the refractory wall of the furnace is of an unknown shape, but the temperature of this surface T_i is assumed to be known and equal to the solidification temperature of the melt, which is recirculating in the furnace. The assumption of the isothermal solidus temperature on the unknown inner surface of the refractory wall is reasonable, although not exact, because there could be layers of solidified melt and slag on some parts of this surface. However, these details could possibly be resolved only by performing a highly accurate conjugate heat transfer analysis [25,26] of the melt flow field and the refractory wall. Despite several attempts at using computational fluid dynamics and conjugate heat transfer analysis [7,12,19,20] to predict shapes of the eroded hearth inner surface, such complex analysis is not sufficiently reliable at the present time because of the stringent requirements on its high accuracy and speed of execution. Hence, the isothermal surface condition on the melt/wall interface is the widely accepted thermal boundary condition.

4 Elastic Membrane Concept for Shape Evolution

Inverse determination of the inner surface shape of the refractory wall of a blast furnace is based on the use of measured T_o and $(dT/dn)_o$ (the overspecified boundary conditions), and on the postulated isothermal value of T_i. These boundary conditions are used in the following manner.

Garabedian and McFadden [27] first proposed the elastic membrane approach for inverse design of aerodynamic shapes, where the body surface is treated as an elastic membrane that deforms under certain surface loads $\Delta C_p(s)$ until it achieves a desired distribution of surface loads. The original nonphysical model for the evolution of, for example, a two-dimensional aerodynamic shape, was given by [27]

$$\beta_0 \Delta n + \beta_1 \frac{d\Delta n}{ds} + \beta_2 \frac{d^2 \Delta n}{ds^2} = \Delta C_p(s) \tag{1}$$

Here, Δn is defined as the shape correction normal to the membrane surface, while the membrane contour-following coordinate

is s. The ordinary differential equation with constant coefficients (Eq. (1)) is analogous to a linear forced spring-damper-mass-spring system, where the monotonically increasing time coordinate has been traded for the surface-contour-following coordinate s. Coefficients β_0, β_1, and β_2 are the user-supplied constants that control the rate of convergence of the iterative shape determination process.

Equation (1) is traditionally solved for shape corrections Δn by evaluating its derivatives using finite differencing. The major problem with this approach is its slow convergence, in conjunction with the field analysis codes of increasing nonlinearity [21]. In an attempt to alleviate these problems, we have developed a new formulation of the elastic membrane design concept, which allows a Fourier series analytical solution to the shape evolution equation [21–24].

4.1 Fourier Series Solution of Shape Evolution Equation. It should be noticed that there is an analogy between the forcing function $\Delta C_p(s)$ in the aerodynamic shape design application, which varies arbitrarily with the contour-following coordinate s and the smelter outer wall surface heat flux difference

$$\Delta q_o = \left(\frac{dT}{dn}\right)_o^{\text{measured}} - \left(\frac{dT}{dn}\right)_o^{\text{computed}} \tag{2}$$

which varies arbitrarily with the circumferential contour-following coordinate θ. Notice also a global periodicity of the mass-damper-spring forcing function and the outer surface heat flux difference Δq_o that repeats its value at the starting and the ending contour-following θ-coordinate.

Thus, on the inner surface of the furnace wall configuration, this elastic membrane surrogate model for inverse shape determination leads to the shape evolution equation [24]

$$\beta_0 \Delta n + \beta_1 \frac{d\Delta n}{d\theta} + \beta_2 \frac{d^2 \Delta n}{d\theta^2} = \Delta q_o \tag{3}$$

which has a homogeneous solution of the general form [24]

$$\Delta n_h = F e^{\lambda_1 \theta} + G e^{\lambda_2 \theta} \tag{4}$$

where F and G are (as yet) undetermined coefficients, and eigenvalues are determined from

$$\lambda_{1,2} = \frac{-\beta_1 \pm \sqrt{\beta_1^2 + 4\beta_0\beta_2}}{-2\beta_2} \tag{5}$$

A particular solution of the elastic membrane model (Eq. (3)) can be represented in terms of a Fourier series as

$$\Delta n_p = A_0 + \sum_{N=1}^{N_{\max}} [A_N \cos N\theta + B_N \sin N\theta] \tag{6}$$

The forcing function Δq_o can also be represented in terms of another Fourier series as

$$\Delta q_o = a_0 + \sum_{N=1}^{N_{\max}} [a_N \cos N\theta + b_N \sin N\theta] \tag{7}$$

Then, from Eq. (6), it follows that

$$\frac{d\Delta n_p}{d\theta} = \sum_{N=1}^{N_{\max}} [-A_N N \cos N\theta + B_N N \sin N\theta] \tag{8}$$

$$\frac{d^2 \Delta n_p}{d\theta^2} = -\sum_{N=1}^{N_{\max}} [A_N N^2 \cos N\theta + B_N N^2 \sin N\theta] \tag{9}$$

Substitution of Eqs. (6), (8), and (9) into the general evolution (Eq. (3)) and collection of like terms yields analytical links among the coefficients of the two Fourier series

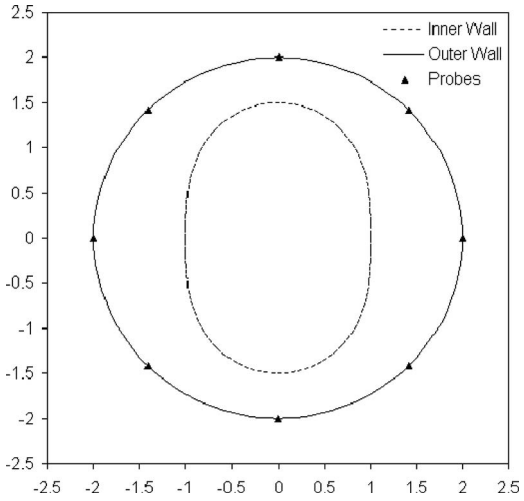

Fig. 1 Symmetric test geometry: target shape of the inner surface (vertical oval) and the outer surface (circle of radius 2.0 m) of the furnace wall with indication of the locations of eight temperature and heat flux probes

$$A_N = \frac{a_N(N^2\beta_2 - \beta_0) - b_N(\beta_1 N)}{(N^2\beta_2 - \beta_0)^2 + (\beta_1 N)^2}, \quad N = 0,1,2,\ldots,N_{\max} \tag{10}$$

$$B_N = \frac{b_N(N^2\beta_2 - \beta_0) + a_N(\beta_1 N)}{(N^2\beta_2 - \beta_0)^2 + (\beta_1 N)^2}, \quad N = 0,1,2,\ldots,N_{\max} \tag{11}$$

Thus, the complete solution for geometry corrections Δn in the locally normal direction to the outside surface of the furnace wall can be represented analytically as

$$\Delta n = F e^{\lambda_1 \theta} + G e^{\lambda_2 \theta} + A_0 + \sum_{N=1}^{N_{\max}} [A_N \cos N\theta + B_N \sin N\theta] \tag{12}$$

The unknown constants, F and G, are determined to be zero from the closure conditions $\Delta n(0) = \Delta n(2\pi)$. This form of solution of the elastic membrane model equation has significant advantages over the standard finite difference approach, since any errors due to finite differencing are removed because the formulation is exact. Consequently, the Fourier series formulation for the elastic membrane concept in inverse shape determination converges faster than the finite difference formulation [21–24].

5 Numerical Results in Horizontal Plane

The Fourier series formulation of the elastic membrane inverse shape determination concept was tested for accuracy and speed of convergence on horizontal cross sections of an idealized furnace, using two simple geometries with outer surface radius $R_o = 2.0$ m. The first test geometry had an oval doubly symmetric inner boundary shape, given as $R_i = 1.0 + 0.5 \sin^2 \theta$ (Fig. 1). The second test geometry had only one axis of symmetry with the inner surface represented by a fourth order polynomial, where slope was discontinuous at the point $R_i(0) = R_i(2\pi)$ (Fig. 2)

$$R_i = 1.0 + 0.5\left\{\left[\frac{(2\pi - \theta)}{2\pi}\right]^4 + \frac{\theta}{2\pi}\right\} \tag{13}$$

Thermal boundary conditions were $T_i = 2000.0$ K and $T_o = 350.0$ K. For simplicity, the furnace wall was assumed to be made of an isotropic homogeneous material. In principle, the analysis of the steady heat conduction could account for a wall made of a finite number of subdomains, each having a different coefficient of thermal conductivity. This is treated easily by the finite element method and could be treated equally easily by the

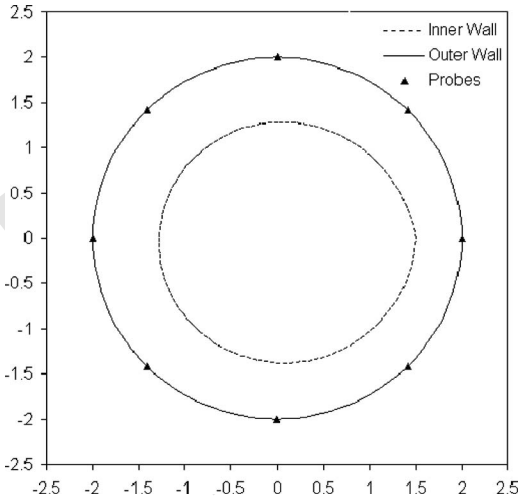

Fig. 2 Asymmetric test geometry: target shape of the inner surface and the outer surface (circle of radius 2.0 m) of the furnace wall with indication of the locations of eight temperature and heat flux probes

boundary element method. Even the realistic situation where the local thermal conductivities are temperature-dependent can be treated relatively easily by both numerical methods [1].

We used a highly accurate boundary element heat conduction analysis code [1] to solve Laplace's equation for a steady thermal field in the annular region. The entire inverse shape determination procedure consisted of the following steps.

1. The "measured" outer surface heat flux corresponding to the inner surface target shape was determined by solving for the temperature field subject to $T_i=2000$ K and $T_o=350$ K, and computing dT/dr on the outer boundary. These boundary values were considered to be errorless.
2. Then, the inner surface was changed to a guessed shape, which was a unit circle in both test cases.
3. Using the analysis code for heat conduction, steady thermal field was solved in this perfectly circular concentric annular region subject to $T_i=2000$ K and $T_o=350$ K.
4. The computed values of dT/dr on the outer boundary were then treated as initial dT/dr computed values.
5. The elastic membrane forcing function Δq_o was then created by the difference between the measured and the initial values of dT/dr on the outer boundary.
6. After several different choices for the values of the elastic membrane coefficients, we used $\beta_0=5000.0$, $\beta_1=0.0$, and $\beta_2=0.0$ that provided the fastest convergence.
7. The inverse design code solved Eq. (3) for corrections in the wall thickness and updated the shape of the inner surface of the furnace wall as $R_i^{\text{new}}=R_i^{\text{old}}+\Delta n$.
8. This shape was then treated as the new initial shape and the entire procedure was automatically repeated.
9. The difference between the computed and the measured heat flux on the outer surface was used as a convergence indicator, and the shape update process was stopped when the heat flux difference reached an acceptably low value (Fig. 3).

The shape of the inner surface of the furnace wall was also used as an indicator of convergence (Fig. 4). After ten iterations in the symmetric test case, the RMS error of dT/dr on the outer surface of the furnace wall decreased to 0.2% of its initial value (Fig. 5), while the RMS error of the radial location of the inner surface decreased to 1.0% of its initial value (Fig. 5).

In the asymmetric geometry test case, the elastic membrane coefficients were chosen as $\beta_0=5000.0$, $\beta_1=0.0$, and $\beta_2=0.0$. After ten iterations, the external surface heat flux difference practically disappeared (Fig. 6), and the inner surface of the furnace wall converged to the target shape (Fig. 7). The RMS error of dT/dr on the outer surface of the furnace wall decreased to 0.1% of its initial value (Fig. 8), while the RMS error on the inner surface of the furnace wall decreased to 0.8% of its initial value (Fig. 8).

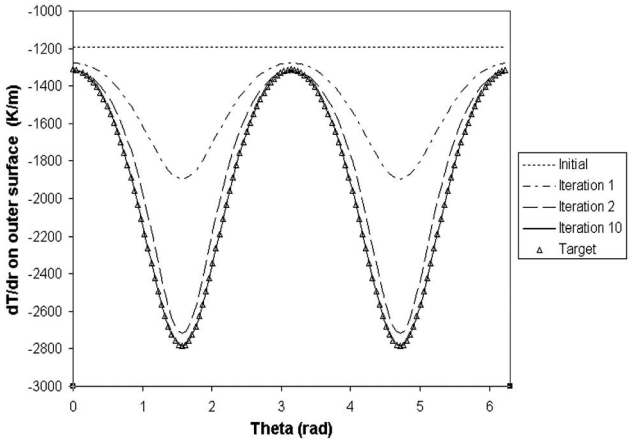

Fig. 3 Symmetric case: convergence history of the outer surface heat flux

6 Effect of Measurement Errors

An actual furnace was not available to evaluate the accuracy of this inverse shape determination method. In an actual field operation of the proposed method, the thermocouples will read local values of temperature on the outer surface of the furnace wall. These readings will inevitably be in error and this error will be randomly distributed among the thermocouples. It is desirable to get maximum information out of as few thermocouples as possible. Consequently, we simulated measurement of the flux at only eight points on the outer surface of the furnace (Figs. 1 and 2). Then, an unbiased error was applied to those eight measurements by using a Gaussian probability distribution (Fig. 9).

These eight randomly perturbed flux values were then spline fitted and interpolated to the remainder of the outer surface of the wall. In a similar fashion, the random error was applied to the computed external temperature, thus simulating actual field measurements with errors. Then, the inverse shape determination procedure was performed while measuring the difference between the

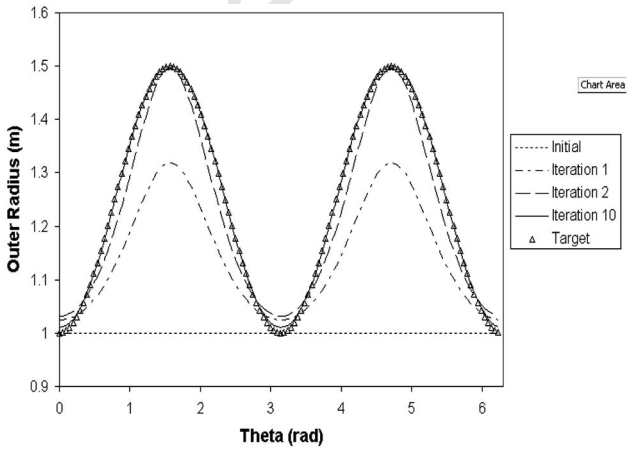

Fig. 4 Symmetric case: convergence history of the inner surface geometry

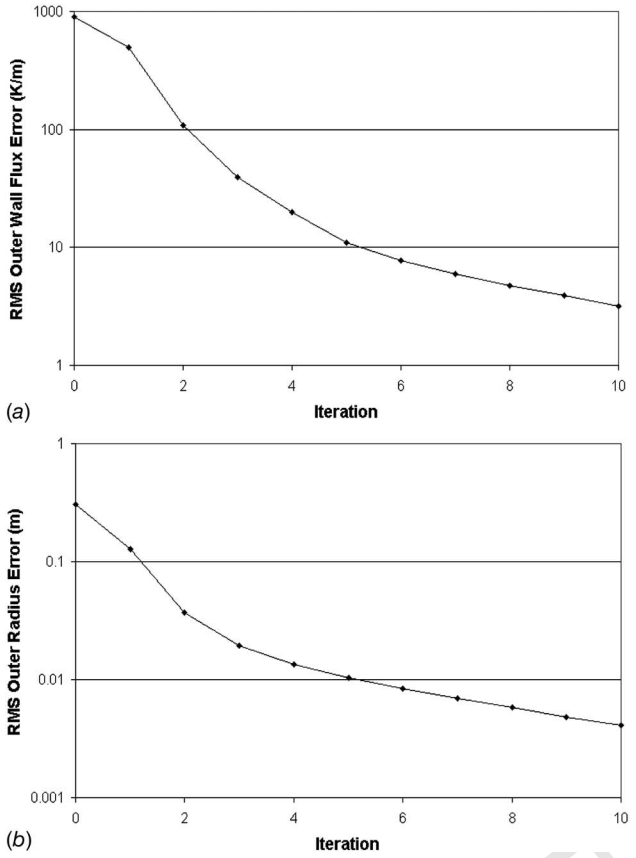

Fig. 5 Symmetric case: convergence history of the RMS error of the outer surface heat flux and of the inner surface geometry

converged shape (subject to the perturbed thermal boundary conditions) and the correct shape. The entire process was repeated a number of times (20 in this case), and the average amount of error in the geometry of the predicted inner surface of the furnace wall was determined.

The effect of different levels of measurement error on the accuracy of furnace inner surface shape prediction is shown in Table 1. The RMS errors, where the average wall thickness used was 0.75 m, were computed as

$$\Delta R_i = (R_i^{\text{target}} - R_i^{\text{predicted}})/(R_o - R_i)_{\text{average}} \qquad (14)$$

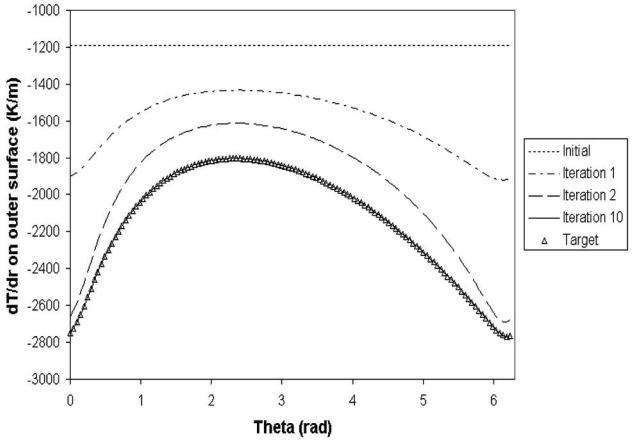

Fig. 6 Asymmetric case: convergence history of the outer surface heat flux

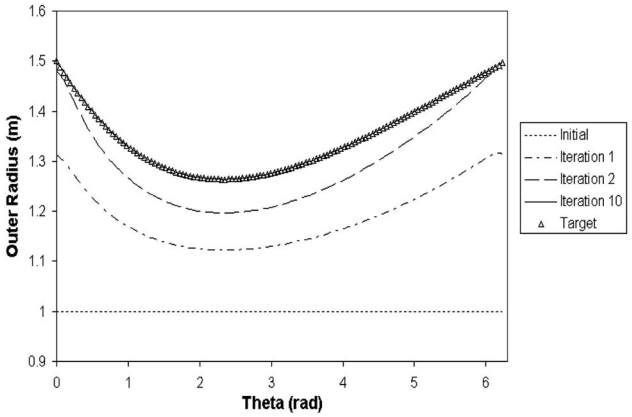

Fig. 7 Asymmetric case: convergence history of the inner surface geometry

7 Numerical Results in Meridional Plane

In the case when the blast furnace configuration is treated as an axisymmetric shape, only half of the vertical (meridional) plane needs to be considered (Figs. 10 and 11). The same elastic membrane concept and Fourier series analytical solution used in the horizontal plane was now applied to the determination of the eroded furnace inner wall shape in the meridional plane.

In this example, there were two material domains: The hearth

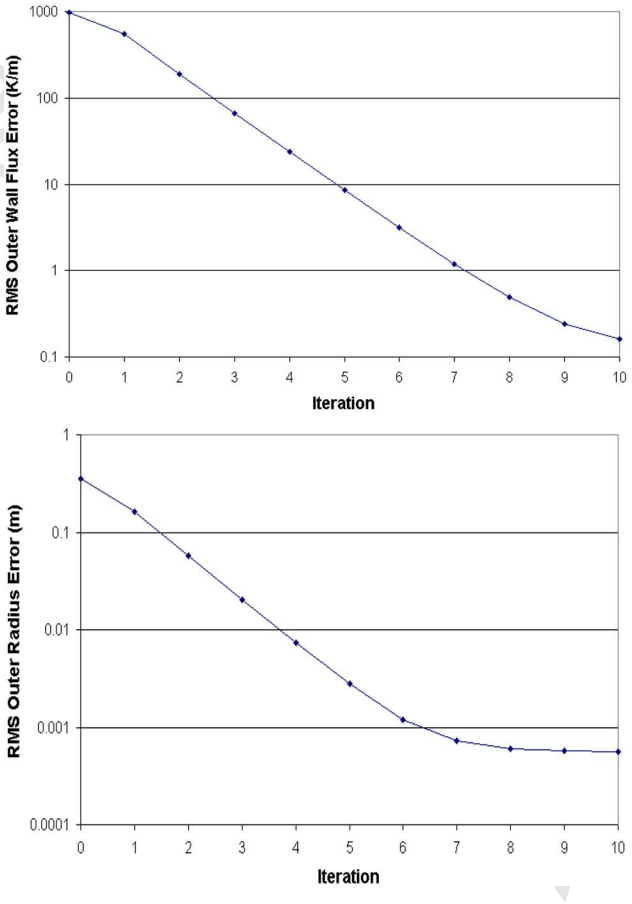

Fig. 8 Asymmetric case: convergence history of the RMS error of the outer surface heat flux and of the inner surface geometry

PROOF COPY [HT-08-1398] 002001JHR

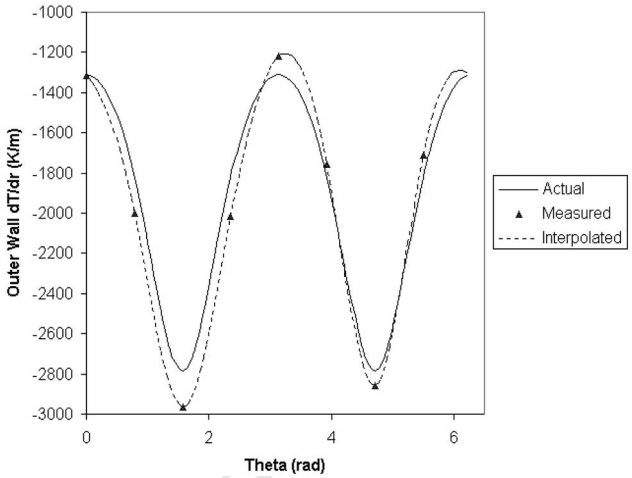

Fig. 9 An example of actual (solid line), measured (actual with stochastically added noise at only eight locations on the outer surface of the furnace wall), and interpolated measured heat fluxes (dashed line) for the geometrically symmetric test case

bottom, 2.5 m of the furnace had thermal conductivity k $=10.0$ W m^{-1} K^{-1}. Everything above that line (i.e., the side wall) had conductivity $k=13.0$ W m^{-1} K^{-1}.

The cold face of the hearth bottom is the furnace bottom surface where natural convective cooling takes place in air, with ambient air temperature assumed to be $T_{air}=310.0$ K and convective heat transfer coefficient was assumed to be h_{air} $=30.0$ W m^{-2} K^{-1}. Temperature probes were assumed to be located at 40 points, spaced evenly in the radial direction on the bottom surface.

The steel shell that contacts the cold face of the hearth sidewall had forced convective cooling by water, where the ambient water temperature was assumed to be $T_{water}=300.0$ K and the convective heat transfer coefficient was assumed to be h_{water} $=150.0$ W m^{-2} K^{-1}. Temperature probes were assumed to be located at 40 points, spaced evenly in the vertical direction on this surface.

The top boundary was treated as thermally insulated. The left boundary is the furnace vertical symmetry line; thus, the boundary condition there was treated as adiabatic.

The curved wall (Figs. 10 and 11) is the melt/furnace interface surface, assumed to be maintained at a constant temperature of $T_i=1720.0$ K.

Here, we used a fast and accurate finite element method [28] to analyze the steady temperature field in the smelter wall. The forcing function in Eq. (3) was the difference between the measured temperatures on the vertical sidewall, on the bottom wall, and on FEM calculated temperatures on these walls. In actual applications, the measured surface temperatures and heat fluxes would be provided at a relatively small number of locations and then interpolated at the larger number (in this example, 40+40=80) surface grid points by using, for example, B-splines.

Inner surface shape corrections were performed along the rays emanating from the imaginary point where the top boundary and furnace centerline intersect. Boundary conditions on Eq. (3) were set, such that $d\Delta n/ds=0$ at the end points so that shape deformation is described with a Fourier cosine series. User-specified coefficients in Eq. (3) were: $\beta_0=200.0$, $\beta_1=0.0$, and $\beta_2=-1.0$, leading to fast and accurate results (Figs. 10–14).

Shape error (Fig. 13) was calculated at 80 evenly spaced points on the design surface (melt-refractory interface) by finding the minimum distances between these points and the target contour (considered to be made up of line segments). RMS and max values are based on that set of 80 individual shape error values.

Temperature errors (Fig. 14) were calculated at each of the 40 evenly spaced points on the vertical sidewall and 40 evenly spaced points on the bottom, as Err$=|T_{calculated}-T_{measured}|$. RMS and max values were based on that set of 80 individual error values.

Table 1 Relative errors in the predicted inner surface radius due to different levels of the simulated measurement errors of temperature and heat flux on the outer surface

Simulated measurement errors		Expected RMS error in predicted values of R_i	
T_o (%)	$(dT/dr)_o$ (%)	Symmetric (%)	Asymmetric (%)
5.0	5.0	4.2	4.9854
0.0	5.0	4.14	4.7852
5.0	0.0	1.21	0.6373
0.0	0.0	0.84	0.6372

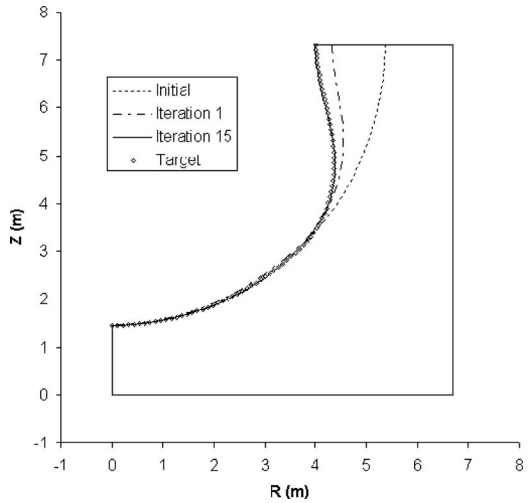

Fig. 10 Initial, target, intermediate, and final shapes of the inner surface of the smelter wall in meridian plane

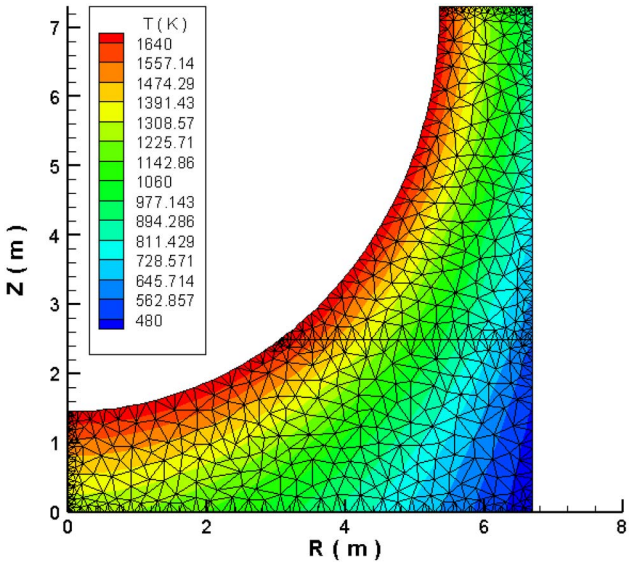

Fig. 11 Initial configuration, temperature field computed using least-squares finite element method [28] and nonstructured computational grid [29]

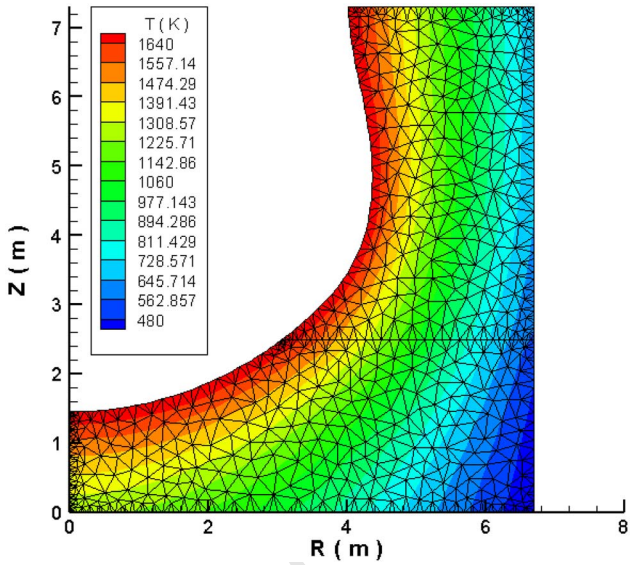

Fig. 12 Final configuration, temperature field computed using least-squares finite element method [28], and computational grid [29]

8 Summary

A new method was developed and tested for the nondestructive determination of wall thickness distribution in blast furnaces and smelters. This technique utilizes external surface measurements of temperature and heat flux and employs a Fourier series solution of an elastic membrane model to evolve the shape of the inner furnace wall. The method accepts any available computer code capable of analyzing the steady temperature field in the furnace wall. It also requires a relatively small number of inexpensive thermocouples. The entire procedure is computationally efficient, highly accurate even under the simulated conditions of measurement noise, and could be extended to the prediction of realistic three-dimensional eroded furnace wall configurations, with sections having different temperature-dependent thermal properties.

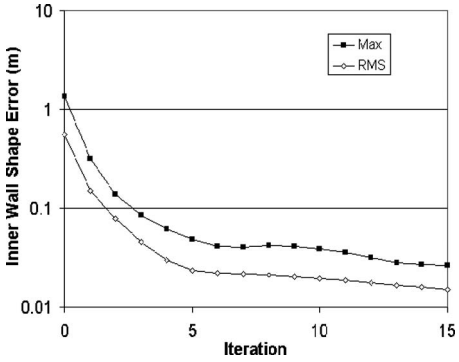

Fig. 13 Convergence history of the inner surface shape error

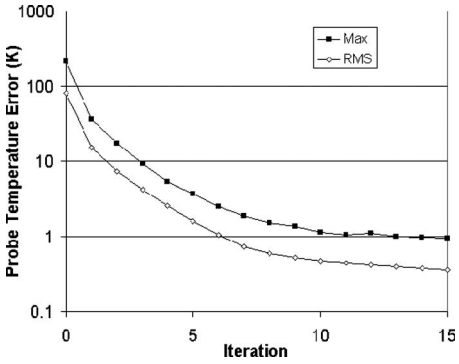

Fig. 14 Convergence history of the inner surface temperature error

Acknowledgment

The authors are grateful for useful comments and suggestions provided by Dr. Keqian (Ken) Liu of U.S. Steel, Technical Center, Monroeville, PA and by the reviewers of the original manuscript. G.S.D. and B.H.D. are grateful for the partial support provided for this research by the U.S. NSF under Grant No. DMS-0073698, administered through the Computational Mathematics program.

Nomenclature

A_N, B_N = Fourier series coefficients for Δn
a_N, b_N = Fourier series coefficients for Δq_o
h = convective heat transfer coefficient (W m^{-2} K^{-1})
k = thermal conductivity (W m^{-1} K^{-1})
N = a term in a Fourier series
n = normal direction to the surface (m)
R = radius of the wall surface (m)
r = radial distance (m)
s = surface-following coordinate (m)
T = temperature (K)
β_0, β_1, β_2 = coefficients in mass-damper-spring model of the elastic membrane
$\Delta C_p(s)$ = difference between target and actual surface pressure (N m^{-2})
Δn = shape correction normal to the surface (m)
Δq_o = outer surface heat flux difference (K m^{-1})
θ = circumferential angle (rad)

Subscript

h = homogeneous part of solution
i = inner surface of the wall
max = maximum number
o = outer surface of the wall
p = particular part of solution

Superscript

old = old (previous) value
new = new (updated) value
target = desired (target) value
predicted = actual (predicted) value

References

[1] Dulikravich, G. S., and Martin, T. J., 1996, "Inverse Shape and Boundary Condition Problems and Optimization in Heat Conduction," *Advances in Numerical Heat Transfer*, W. J. Minkowycz and E. M. Sparrow, eds., Taylor & Francis, London, Vol. 1, pp. 381–426.

[2] Dennis, B. H., and Dulikravich, G. S., 1999, "Simultaneous Determination of Temperatures, Heat Fluxes, Deformations, and Tractions on Inaccessible Boundaries," ASME J. Heat Transfer, **121**, pp. 537–545.

[3] Yoshikawa, F., and Szekely, J., 1981, "Mechanism of Blast Furnace Hearth Erosion," Ironmaking Steelmaking, **8**, pp. 159–168.

[4] Yoshikawa, H., et al., 1984, "Estimation of Erosion Line of Refractory and Solidification Layer in Blast Furnace Hearth," *Proceedings of the Fourth Conference on Simulation Technology*, Japan Society for Simulation Technology, pp. 75–78.

[5] Yoshikawa, F., Nigo, S., Kiyohara, S., Taguchi, S., Takahashi, H., and Ichimiya, M., 1987, "Estimation of Refractory Wear and Solidified Layer Distribution in the Blast Furnace Hearth and Its Application to the Operation," Tetsu to Hagane, **73**(15), pp. 2068–2075.

[6] Shin, M., and Lee, J.-W., 2000, "Prediction of the Inner Wall Shape of an Eroded Furnace by the Nonlinear Inverse Heat Conduction Technique," JSME Int. J., Ser. B, **43**(4), pp. 544–549.

[7] Takatani, K., Inada, T., and Takata, K., 2001, "Mathematical Model for Transient Erosion Process of Blast Furnace Hearth," ISIJ Int., **41**(10), pp. 1139–1145.

[8] Matsevity, Y. M., Moultanovsky, A. V., and Nemirovsky, I. A., 1988, "Simu-

lation of Thermal State Discretely Cooled Constructions of Units of Non-Ferrous Metallurgy," Promenergetika, **1**, pp. 42–44.

[9] Matsevity, Y. M., Moultanovsky, A. V., and Timchenko, V. M., 1991, "Diagnostics of Destruction of Cooled Caisson Wall Units on the Base of Identification of Heat Transfer Conditions," Promyshlennaya Teplotekhnika, **13**(3), pp. 3–12.

[10] Kostikov, A. O., and Matsevity, Y. M., 1998, "Determination of Thickness of Heat Transferring Wall With the Help of Solving Geometrical Inverse Heat Conduction Problem," Problemy Mashinostroeniya, **1**(3–4), pp. 52–59.

[11] Matsevity, Y. M., Timchenko, V. M., and Kostikov, A., 2001, "Identification of Destruction in Metallurgical Equipment by Solving the Inverse Heat Conduction Problems," *Proceedings of the ICHMT Symposium CHT'01—Advances in Computational Heat Transfer*, Davis G. de Vahl and E. Leonardi, eds., Begell House Inc., New York, Vol. 2, pp. 1145–1152.

[12] Preuer, A., Winter, J., and Hiebler, H., 1992, "Computation of the Erosion in the Hearth of a Blast Furnace," Steel Res., **63**(4), pp. 147–151.

[13] Druckenthaner, H., et al., 1998, "Online Simulation of the Blast Furnace," *Advanced Steel*, pp. 58–61.

[14] Radmoser, E., 1998, "Security-Related Parts of a Blast Furnace Model," ECMI Newsletter No. 23.

[15] Sorli, K., and Skaar, I. M., 1999, "Monitoring the Wear-Line of a Melting Furnace," *Proceedings of the 3ICIPE, Third International Conference on Inverse Problems in Engineering*, K. Woodbury, ed., ASME, New York.

[16] Tanaka, M., Matsumoto, T., and Oida, S., 1998, "Identification of Unknown Boundary Shape of Rotationally Symmetric Body in Steady Heat Conduction Via BEM and Filter Theories," *Inverse Problems in Engineering Mechanics—ISIP '98*, M. Tanaka, and G. S. Dulikravich, eds., Elsevier, New York pp. 121–130.

[17] Tanaka, M., Matsumoto, T., and Yano, T., 2000, "A Combined Use of Experimental Design and Kalman Filter-BEM for Identification of Unknown Boundary Shape for Axisymmetric Bodies Under Steady-State Heat Conduction," *Proceedings of the Inverse Problems in Engineering Mechanics—ISIP '00*, M. Tanaka and G. S. Dulikravich, eds., Elsevier, New York pp. 3–12.

[18] Katamine, E., Azegami, H., and Kojima, M., 1999, "Boundary Shape Determination on Steady-State Heat Conduction Fields," JSME Int. J., Ser. B, **65**(629), pp. 275–281.

[19] Huang, D., Chaubal, P., Abramowitz, H., and Zhou, C., 2005, "Hearth Skulls and Hearth Wear Investigation of ISPAT Inland's #7 Blast Furnace," *Proceedings of the AIST 2005*, Charlotte, NC, Vol. 1, pp. 101–112.

[20] Roldan, D., 2005, "Numerical Investigation of the Erosion in a Blast Furnace Hearth," MS thesis, Purdue University Calumet, IN.

[21] Dulikravich, G. S., and Baker, D. P., 1998, "Fourier Series Analytical Solution for Inverse Design of Aerodynamic Shapes," *Inverse Problems in Engineering Mechanics—ISIP '98*, M. Tanaka and G. S. Dulikravich, eds., Elsevier, UK, pp. 427–436.

[22] Dulikravich, G. S., and Baker, D. P., 1999, "Using Existing Flow-Field Analysis Codes for Inverse Design of Three-dimensional Aerodynamic Shapes," *Recent Development of Aerodynamic Design Methodologies—Inverse Design and Optimization*, K. Fujii and G. S. Dulikravich, eds., Vol. 68, Springer, New York, pp. 89–112.

[23] Baker, D. P., 1999, "A Fourier Series Approach to the Elastic Membrane Inverse Shape Design Problem in Aerodynamics," MS thesis, Department of Aerospace Engineering, Pennsylvania State University, University Park, PA.

[24] Baker, D. P., Dulikravich, G. S., Martin, T. J., and Dennis, B. H., 2003, "Inverse Determination of Smelter Wall Erosion Shapes Using a Fourier Series Method," *Proceedings of the International Symposium on Inverse Problems in Engineering Mechanics—ISIP '03*, Nagano, Japan, Feb. 18–21.

[25] Han, Z.-X., Dennis, B. H., and Dulikravich, G. S., 2001, "Simultaneous Prediction of External Flow-Field and Temperature in Internally Cooled 3-D Turbine Blade Material," Int. J. Turbo Jet Engines, **18**(1), pp. 47–58.

[26] Dulikravich, G. S., 1999, "Electro-Magneto-Hydrodynamics and Solidification," *Advances in Flow and Rheology of Non-Newtonian Fluids, Part B*, D. A. Siginer, D. De Kee, and R. P. Chhabra, eds., Elsevier, New York, Vol. 8, pp. 677–716.

[27] Garabedian, P., and McFadden, G., 1982, "Design of Supercritical Swept Wings," AIAA J., **20**(3), pp. 289–291.

[28] Dennis, B. H., Eberhart, R. C., Dulikravich, G. S., and Radons, S. W., 2003, "A Finite Element Simulation of Cooling of 3-D Human Head and Neck," J. Biomech. Eng., **125**, pp. 832–840.

[29] Marcum, D. L., and Weatherhill, N. P., 1995, "Unstructured Grid Generation Using Iterative Point Insertion and Local Reconnection," AIAA J., **33**(9), pp. 1619–1625.

PROOF COPY [HT-08-1398] 002001JHR

AUTHOR QUERIES — 002001JHR

#1 AU: Please check insertion of heading "Introduction" for this section.

#2 AU: All figures must be cited in numerical order in text. Fig. 9 was not cited in text. Please check our insertion here.

#3 AU: Please check our edits in the Acknowledgment.

#4 AU: "et al." is not allowed in the references. Please supply the full list of authors for Refs. 4 and 13.

#5 AU: Please verify change to journal title for Ref. 6.

#6 AU: Please supply full journal title, the coden, and/or ISSN for Refs. 8, 9, and 10.

#7 AU: Please supply full journal title, the coden, and/or ISSN for Ref. 9.

#8 AU: Please verify the year and provide publisher name and city if this is a book for Ref. 13.